

Ab Initio Study of the H₂ Elimination from CH₂OH⁺, CH₂NH₂⁺, and CH₂SH⁺

D. Suárez and T. L. Sordo*

Departamento de Química Física y Analítica, Facultad de Química, Universidad de Oviedo, C/ Julián Clavería, 8, 33006 Oviedo, Principado de Asturias, Spain

Received: September 9, 1996; In Final Form: November 15, 1996[⊗]

The potential energy surfaces (PESs) of H₂CXH_n⁺ (X = O, n = 1; X = N, n = 2; X = S, n = 1) systems were investigated by using the ab initio method at MP2/6-311+G** and QCISD/6-311+G** levels, and single-point calculations on the MP2 and the QCISD geometries were performed at the QCISD(T)/6-311+G-(3df,2p) level. At the QCISD(T)/6-311+G(3df,2p)//MP2/6-311+G** level including ZPVE correction from MP2/6-311+G** unscaled frequencies, the proton affinities are 168.9, 207.2, and 182.9 kcal/mol for formaldehyde, formaldimine, and thioformaldehyde, respectively, while the energy barriers and reaction energies for hydrogen 1,2-elimination from the corresponding protonated systems are 79.3 and 22.0, 90.3 and 42.2, and 61.9 and 27.9 kcal/mol, respectively. Hydrogen 1,1-eliminations are not competitive compared with 1,2-eliminations. The reaction path for hydrogen 1,2-elimination from protonated formaldehyde goes through planar structures, whereas those from protonated formaldimine and thioformaldehyde involve rotation about the C–X double bond. The hydrogen 1,2-elimination takes place through a concerted mechanism for protonated formaldehyde and formaldimine, whereas for protonated thioformaldehyde a two-step mechanism was found on the electronic PES. By taking account of the ZPVE correction, a concerted mechanism results. For protonated thioformaldehyde a TS for proton scrambling was found about 5 kcal/mol more stable than the TS for hydrogen 1,2-elimination (this energy difference remains even at the QCISD(T)/6-311+G(3df,2p)//MP2/6-311+G(3df,2p) level). This result is in contrast with deuterium label experiments.

Introduction

An important characteristic of unimolecular decompositions is the energy released as relative motion between the fragments.¹ The relative amount of kinetic energy released is determined by the dynamics of the process and therefore constitutes a probe of the shape of the potential energy surface (PES) in the exit valley.

Large translational energy releases have been experimentally observed for many eliminations of H₂ from small organic ions.² The processes for CH₂OH⁺, CH₂NH₂⁺, and CH₂SH⁺ have been experimentally established to be concerted 1,2-eliminations occurring with release of 33 (41.5 or 42.9 kcal/mol,³ and 37.6 kcal/mol⁴ according to subsequent determinations), 20 (24.4 kcal/mol⁵), and 20 kcal/mol, respectively.² It has been proposed that these three H₂ elimination reactions proceed via concerted symmetry-forbidden routes in such a way that intended crossings are avoided and, as a consequence, kinetic energy is released.

In a theoretical study³ of the dynamics of H₂ elimination from protonated formaldehyde it has been shown by quantum chemical calculations that H₂ does not depart from CH₂OH⁺ in a symmetrical fashion. The transition structure (TS) geometry found agrees well with the experimental finding that the reaction is a concerted 1,2-elimination. The classical trajectory calculated from the located TS to separate products reproduces the experimentally observed translational energy release and the isotope effects. The translational energy release is a complicated function of the motion along the whole reaction trajectory. Very recently, Kim et al.⁴ have reported new measurements and classical calculations of the kinetic energy release (KER) distribution for this process. On the basis of their detailed dynamical calculations, they have found that the strained bending forces at the TS and the strengthening of the C–O bond from double to triple character were mainly responsible for the significant KER.

In a theoretical study⁵ of the dynamics of methaniminium cation a 1,1-elimination TS was located by means of ab initio calculations. A good agreement has been found between the experimental energy release distribution and that calculated using the located TS, although significant disagreement has resulted in the case of isotope effects. The 1,1-elimination TS geometry was then adjusted to give an exact fit to the experimental energy release, the adjusted geometry became completely asymmetric, and the departing H atoms were nonequivalent. To our knowledge no theoretical study of hydrogen elimination from protonated thioformaldehyde has been carried out.

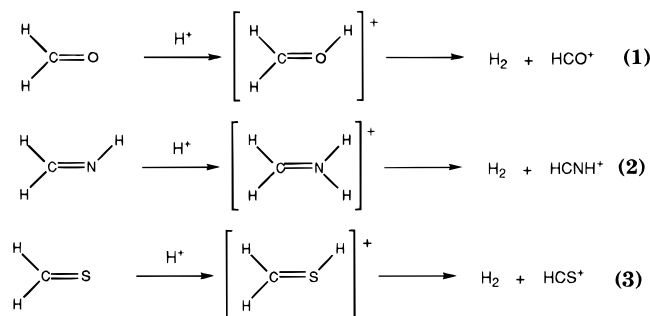
Although the full explanation of the kinetic energy release would require a study of the dynamics of the process, it is clear that that goal cannot be achieved without a precise knowledge of the corresponding PES. Thus a detailed study of the most significant stable structures and TSs connecting them on the PES corresponding to several unimolecular decompositions presenting an important KER seems valuable in order to get a deeper knowledge of the features determining their dynamical behavior. In this work we present a comparative study of high-level ab initio PESs of protonated formaldehyde, formaldimine, and thioformaldehyde, focusing our attention on protonation, H₂ elimination, and hydrogen scrambling processes.

Methods

Ab initio calculations were performed with the Gaussian 92 series of programs.⁶ Stable species were fully optimized and TSs located using Schelgel's algorithm⁷ at the MP2/6-311+G** theory level. All the critical points were further characterized, and the ZPVE was evaluated by analytical computations of harmonic frequencies at the MP2/6-311+G** level. Thermodynamic gas-phase magnitudes were computed to obtain results more readily comparable with experiment within the ideal gas, rigid rotor, and harmonic oscillator approximations.⁸ In addi-

[⊗] Abstract published in *Advance ACS Abstracts*, January 1, 1997.

SCHEME 1



tion, the most important structures were also optimized at the QCISD/6-311+G** theory level. Single-point calculations on the MP2 and QCISD geometries were also carried out at the QCISD(T)/6-311+G(3df,2p) level. The frozen core approximation was used in all the correlated calculations.

Reaction paths passing through the main TS located in this work were studied by MP2/6-311+G** intrinsic reaction coordinate (IRC) calculations using the Gonzalez and Schlegel⁹ method implemented in Gaussian 92.

Molecular properties and total electronic density, ρ , computed at the MP2/6-311+G** level were used to interpret the computational results. Following the method of Bader,¹⁰ we have carried out a topological analysis of the (3, -1) bond critical points (BCPs) in ρ . The BCP analysis employed the program EXTREME, a part of the AIMPACK suite of programs.¹¹ The PROAIM program was used to compute integrated atomic charges according to atoms-in-molecules type decomposition of the electronic density.

Coupling constants $B_{s,k}$ between normal coordinates and the reaction coordinate were computed at the TS according to the definition proposed by Handy et al.¹²

$$B_{s,k} = \mathbf{L}_s^T \left(\frac{\partial \mathbf{L}_k}{\partial s} \right) = -\mathbf{L}_k^T \left(\frac{\partial \mathbf{L}_s}{\partial s} \right) \quad (1)$$

where \mathbf{L}_s and \mathbf{L}_k are the unitary vectors associated with the reaction coordinate s and mode k in mass-weighted Cartesian coordinates, respectively. $B_{s,k}$ represents the direct coupling between the reaction coordinate and the various k normal modes induced by motions along the reaction coordinate. The derivative of mode k with respect to the reaction coordinate could be calculated by numerical differentiation. This procedure is equivalent to differencing both the second-order and third-order contributions of the energy derivatives to the coupling constants. A better estimation of the coupling constants can be obtained using analytic formulas which have important computational advantages over finite difference techniques:¹³

$$B_{s,k} = -\mathbf{L}_k^T (2\mathbf{L}_s^T \mathbf{F} \mathbf{L}_s \mathbf{I} - \mathbf{F})^{-1} \left(\frac{\partial \mathbf{F}}{\partial s} - \mathbf{L}_s^T \frac{\partial \mathbf{F}}{\partial s} \mathbf{L}_s \mathbf{I} \right) \mathbf{L}_s \quad (2)$$

where \mathbf{F} is the Hessian matrix. In the present work eq 2 was evaluated by computing third-order contributions by numerical differentiation using a central difference formula within a small displacement (0.01 amu^{1/2} bohr) along s .

Results

The protonations of formaldehyde, formaldimine, and thioformaldehyde and the mechanism of H₂ elimination from the resulting cations have been investigated by means of the ab initio method. See Scheme 1.

Figures 1–4 display the structural features resulting from the geometry optimizations of the most important critical points for

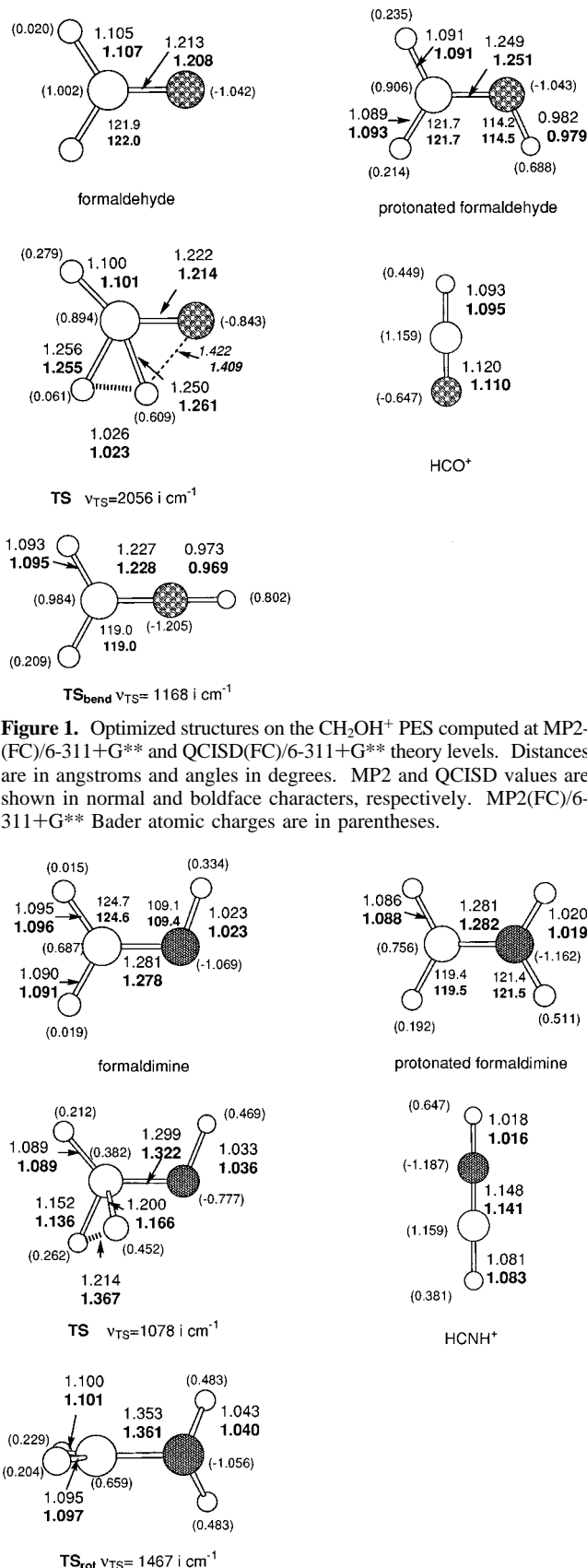


Figure 1. Optimized structures on the CH₂OH⁺ PES computed at MP2-(FC)/6-311+G** and QCISD(FC)/6-311+G** theory levels. Distances are in angstroms and angles in degrees. MP2 and QCISD values are shown in normal and boldface characters, respectively. MP2(FC)/6-311+G** Bader atomic charges are in parentheses.

Figure 2. Optimized structures on the CH₂NH₂⁺ PES computed at MP2(FC)/6-311+G** and QCISD(FC)/6-311+G** theory levels. Distances are in angstroms and angles in degrees. MP2 and QCISD values are shown in normal and boldface characters, respectively. MP2-(FC)/6-311+G** Bader atomic charges are in parentheses.

processes 1–3. Figure 5 sketches the reaction coordinate, the normal modes, and their coupling constants with the reaction

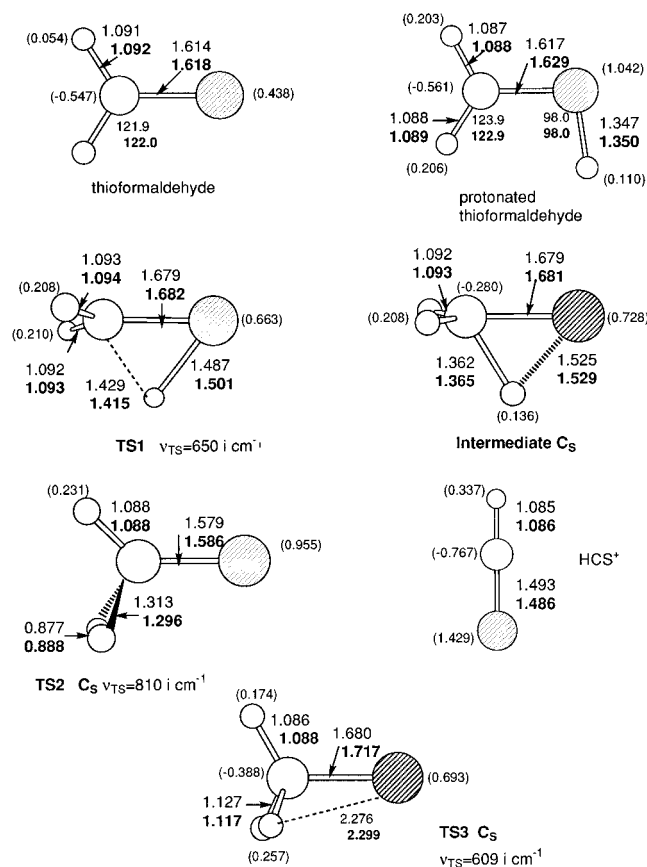


Figure 3. Optimized structures on the CH₂SH⁺ PES computed at MP2-(FC)/6-311+G** and QCISD(FC)/6-311+G** theory levels. Distances are in angstroms and angles in degrees. MP2 and QCISD values are shown in normal and boldface characters, respectively. MP2(FC)/6-311+G** Bader atomic charges are in parentheses (some atomic charges are not shown due to a poor numerical integration).

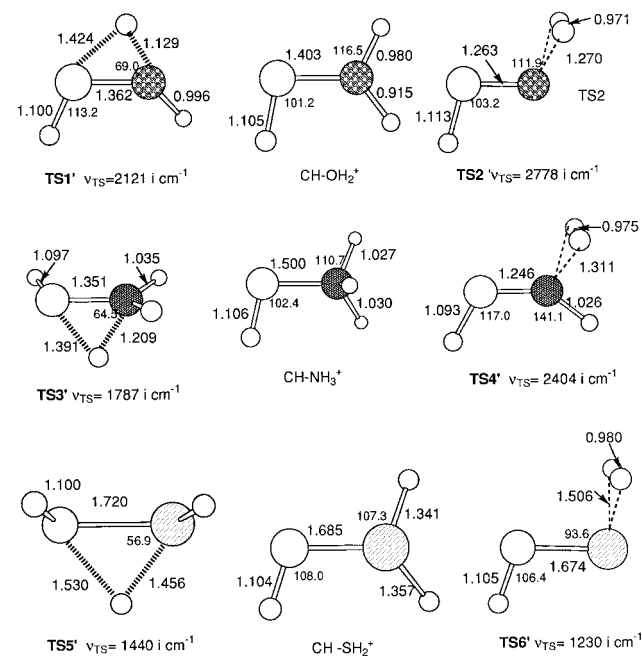


Figure 4. Minima and transition structures corresponding to the H₂ 1,1-elimination through CHX₂⁺ intermediates (X = O, NH, S) computed at the MP2(FC)/6-311+G** level. Distances are in angstroms and angles in degrees.

coordinate at the TS for H₂ elimination from protonated formaldehyde.

Tables 1–3 collect the relative energies of the structures

TABLE 1: Relative Energies (kcal/mol) with Respect to CH₂XH⁺ Minima (X = O, NH, S) of the Main Structures Considered in This Work; Geometries Optimized at the MP2(FC)/6-311+G Level**

structures	MP2	ZPVE ^a	QCISD(T) ^b	ΔH ^c	ΔG ^c
CH ₂ O + H ⁺	175.8	-10.9	177.1	168.9	161.8
TS H ₂ 1,2-elimination	86.0	-8.3	87.6	81.3	81.0
CHO ⁺ + H ₂	27.3	-11.1	33.1	25.6	18.2
TS _{Bend}	24.3	-4.4	23.8	21.5	21.2
CH ₂ NH + H ⁺	214.5	-10.9	214.8	207.2	199.3
TS H ₂ 1,2-elimination	99.6	-7.2	97.6	92.2	91.7
CHNH ⁺ + H ₂	51.1	-12.3	54.5	46.0	38.0
TS _{Rot}	73.7	-5.7	72.4	68.6	68.6
CH ₂ S + H ⁺	188.8	-6.8	188.4	182.9	175.9
TS1	49.8	-2.5	50.1	47.6	47.6
intermediate	49.6	-1.9	50.1	48.4	48.2
TS2 H ₂ 1,2-elimination	66.0	-4.1	66.0	62.0	61.8
CHS ⁺ + H ₂	29.6	-7.2	35.1	29.7	22.3
TS3 proton scrambling	62.7	-2.3	59.1	56.8	56.7

^a ZPE correction computed at the MP2(FC)/6-311+G** level. ^b QCISD(T)(FC)/6-311+G(3df,2p)//MP2(FC)/6-311+G**. ^c 298.15 K, 1 atm using QCISD(T) electronic energies and MP2/6-311+G** frequencies.

TABLE 2: Relative Energies (kcal/mol) with Respect to CH₂XH⁺ Minima (X = O, NH, S) of the Main Structures Considered in This Work; Geometries Optimized at the QCISD(FC)/6-311+G Level**

structures	QCISD	QCISD(T) ^a
CH ₂ O + H ⁺	179.6	177.0
TS H ₂ 1,2-elimination	91.0	87.6
CHO ⁺ + H ₂	31.9	33.0
TS _{Bend}	24.7	23.9
CH ₂ NH + H ⁺	217.4	214.8
TS H ₂ 1,2-elimination	98.2	96.8
CHNH ⁺ + H ₂	54.6	54.4
TS _{Rot}	72.6	72.4
CH ₂ S + H ⁺	193.2	188.4
TS1	50.8	50.2
intermediate	50.7	50.1
TS2 H ₂ 1,2-elimination	68.7	66.0
CHS ⁺ + H ₂	35.2	35.1
TS3 proton scrambling	59.6	58.7

^a QCISD(T)(FC)/6-311+G(3df,2p)//QCISD(FC)/6-311+G**.

TABLE 3: Relative Energies (kcal/mol) of the Structures (TS and Minima) on the MP2(FC)/6-311+G PES for the 1,1-Elimination of H₂ from CHX₂⁺ Intermediates; The Values Are Given with Respect to the Corresponding CH₂XH⁺ Minima (X = O, NH, S)**

structure	MP2	ZPVE ^a	QCISD(T) ^b
TS1' proton scrambling	112.3	-7.6	110.0
CHOH ₂ ⁺	81.7	-3.5	79.2
TS2' H ₂ 1,1-elimination	167.7	-10.9	158.2
TS3' proton scrambling	114.6	-5.9	112.3
CHNH ₃ ⁺	96.4	-4.2	92.5
TS4' H ₂ 1,1-elimination	157.9	-9.5	151.6
TS5' proton scrambling	107.8	-4.9	102.5
CHSH ₂ ⁺	90.3	-3.4	83.5
TS6' H ₂ 1,1-elimination	126.0	-5.7	118.0

^a ZPE correction computed at the MP2(FC)/6-311+G** level. ^b QCISD(T)(FC)/6-311+G(3df,2p)//MP2(FC)/6-311+G**.

considered in this work computed at different theory levels. Unless otherwise specified the relative energies given in the text hereafter correspond to the QCISD(T)/6-311+G(3df,2p)//MP2/6-311+G** level including ZPVE correction from the MP2/6-311+G** unscaled frequencies. BCP properties of the most important TS are presented in Table 4.

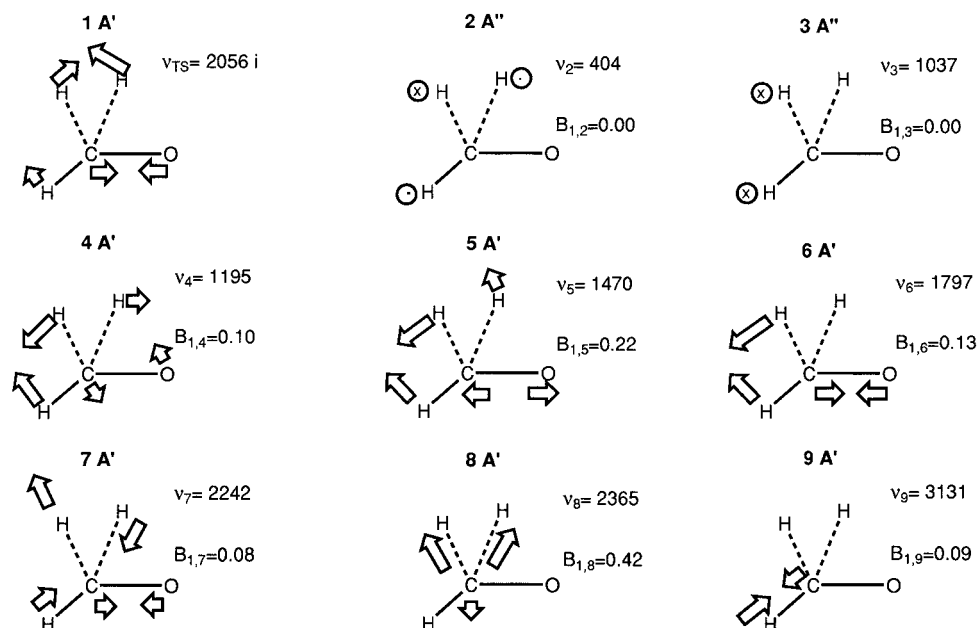


Figure 5. Sketch of the normal modes corresponding to the TS for H₂ 1,2-elimination from protonated formaldehyde obtained at the MP2(FC)/6-311+G** level. Harmonic frequencies are given in cm⁻¹. Coupling constants ($B_{1,i}$ in amu^{1/2} bohr) of normal modes with reaction coordinates are also indicated.

TABLE 4: Bond Critical Point Properties^a (au) of the Main Transition Structures Optimized in This Work at the MP2(FC)/6-311+G Level**

	$\rho(r_c)$	$\nabla^2\rho(r_c)$	ϵ	r_1	r_2	$H(r_c)$
C–O	0.399	-0.106	0.170	0.786	1.524	-0.677
C–H _a	0.175	-0.324	1.655	1.734	0.710	-0.138
C–H _b	0.205	-0.483	0.687	1.548	0.933	-0.165
C–H _c	0.280	-1.061	0.024	1.435	0.645	-0.289
C–N	0.367	-0.925	0.218	0.878	1.578	-0.585
C–H _a	0.181	-0.429	0.457	1.551	0.722	-0.157
C–H _b	0.234	-0.690	0.222	1.446	0.736	-0.214
C–H _c	0.285	-1.052	0.017	1.393	0.665	-0.293
N–H	0.326	-1.756	0.033	1.475	0.477	-0.487
C–S	0.243	0.313	0.306	1.834	0.150	-0.301
C–H	0.284	-1.046	0.033	1.398	0.658	-0.292
H–H	0.203	-0.584	0.656	0.857	0.857	-0.173
C– $\sigma_{(H_2)}$	0.174	-0.237	1.737	1.345	1.294	-0.131
C–S	0.232	-0.528	0.047	1.540	1.635	-0.214
C–H _a	0.284	-1.020	0.005	1.373	0.679	-0.290
C–H _b	0.239	-0.738	0.073	1.422	0.708	-0.225

^a $\rho(r_c)$, $\nabla^2\rho(r_c)$, and ϵ stand for the electronic density, Laplacian of the electronic density, and ellipticity at BCP, respectively. r_1 and r_2 are the distances from the critical point to A and B in the bond A–B. $H(r_c)$ is the local energy density: $H(r_c) = G(r_c) + V(r_c)$ (see ref 16).

Formaldehyde. The proton affinity of formaldehyde obtained in this work is 168.9 kcal/mol (see Table 1), which is close to the experimental value of 170 kcal/mol.¹⁴ The charge transfer from formaldehyde to the attached proton is only 0.312e. The electronic population of the oxygen atom remains nearly unaltered.

Concerning the H₂ elimination, our results agree with previous theoretical studies^{3,4} predicting a concerted mechanism through a planar TS which shows a nonsymmetrical departure of the hydrogen molecule (see Figure 1). Geometrical and BCP analyses clearly show that the atoms of the emerging hydrogen molecule present a three-center interaction with the carbon atom. In effect, according to MP2 calculations, the two C–H distances are 1.256 and 1.250 Å, whereas the shortest O–H distance is 1.422 Å (see Figure 1). No BCP appears between O and H (see Table 4). Furthermore, the analysis of normal modes of vibration of this TS confirms the three-center interaction through the presence of the symmetric and antisymmetric vibrations of the CH₂ moiety (see Figure 5). It is also interesting to note that the strengthening of the C–O bond from double-bond to triple-bond character occurs mostly after the TS (see Figure 1 and Table 4). An IRC calculation starting at this TS shows that this H₂ elimination takes place maintaining C_s symmetry along the reaction path.

The computed activation energy and reaction energy for this 1,2-elimination are, respectively, 79.3 and 22.0 kcal/mol. These values are in good agreement with the experimental data reported by Ugerrud³ (77.9 and 26.1 kcal/mol) and more recently by Kim⁴ (77.5 and 27.7 kcal/mol).

A TS was also located connecting protonated formaldehyde and its mirror image (see Figure 1). This process implies an in-plane large amplitude bending motion of the attached proton about the C–O bond. This in-plane motion does not affect the C–O bond and presents an energy barrier of only 19.4 kcal/mol.

Optimizations of the studied structures at the QCISD/6-311+G** theory level render geometries very similar to the MP2 ones (see Figure 1). Furthermore, from Tables 1 and 2 we see that single-point calculations at the QCISD(T)/6-311+G-(3df,2p) theory level on MP2 and QCISD geometries give completely coincident relative energies for this system.

For completeness proton scrambling and H₂ 1,1-elimination via the CHOH₂⁺ singlet intermediate were also studied (see Figure 4 and Table 3). This intermediate is 75.7 kcal/mol less stable than protonated formaldehyde as a consequence of the loss of double-bond character of C–O and the resultant carbene

structure. The TS for proton transfer from C to O leading to CHOH₂⁺ and for H₂ 1,1-elimination are, respectively, 102.4 and 147.2 kcal/mol above protonated formaldehyde. These two processes then are unfavored with respect to the H₂ 1,2-elimination, in agreement with deuterium labeling experiments.

Formaldimine. The calculated proton affinity (PA) of formaldimine is 207.2 kcal/mol (see Table 1), in reasonable agreement with the experimental value of 202.3 kcal/mol.¹⁵ The charge transfer to the proton amounts in this case to 0.489e, the electronic population of the nitrogen atom remaining unaltered.

In the case of the decomposition of CH₂NH₂⁺, MO calculations render also a concerted mechanism through a nonplanar nonsymmetrical TS (see Figure 2). From the geometry and BCP data corresponding to this TS we perceive again a three-center interaction between the two leaving H atoms and the C atom. According to MP2 calculations the two C–H distances are 1.200 and 1.152 Å, and the distance of the breaking N–H bond is 1.660 Å (see Figure 2). No BCP was found between N and the departing H atom (see Table 4). The normal mode analysis of this system (not presented here) reflects again a three-center interaction. The strengthening of the C–N bond from double to triple character takes place after the TS (see bond distances in Figure 2; the MP2 electron density at the BCP for C–N in the TS is 0.367 au; the corresponding value in the product HCNH⁺ is 0.448 au).

The computed activation and reaction energies are, respectively, 90.3 and 42.2 kcal/mol. Williams and Hvistendahl report an activation energy of 97 kcal/mol.²

A TS connecting protonated formaldimine with its mirror image was found (see Figure 2). This TS corresponds to a rotation about the C–N bond, which implies a partial loss of the double-bond character. This motion is energetically costly, rendering a barrier of 67.4 kcal/mol.

From Figure 2 and Tables 1 and 2 we see again that calculations at the QCISD(T)/6-311+G(3df,2p)//QCISD/6-311+G** theory level render geometries and relative energies very similar to the QCISD(T)/6-311+G(3df,2p)/MP2/6-311+G** ones.

In the study of proton scrambling from C to N leading to CHNH₃⁺ and subsequent H₂ 1,1-elimination the corresponding TSs are, respectively, 106.5 and 142.1 kcal/mol above protonated formaldimine. This route then is not competitive compared with the previously discussed H₂ 1,2-elimination, in accordance with deuterium labeling experiments.

Thioformaldehyde. The PA of thioformaldehyde obtained with our calculations is 182.9 kcal/mol, comparable with the experimental value of 185 kcal/mol.¹⁴ The charge transfer from thioformaldehyde to the attached proton amounts to 0.890e. From Figure 3 we see that in this case the electronic rearrangement involved in the protonation on sulfur appreciably affects this atom, while the electronic density of the C atom remains practically unaltered.

Concerning the 1,2-elimination of H₂ from thioformaldehyde, it was found that the reaction proceeds along a two-step mechanism on both MP2/6-311+G** and QCISD/6-311+G** electronic energy surfaces. The first TS located along the reaction path, TS1, corresponds to a rotation about the C–S bond (see Figure 3) and is 47.2 kcal/mol less stable than protonated thioformaldehyde (see Table 1). TS1 leads to a C_s intermediate which is a π complex structure between the proton and thioformaldehyde (see Figure 3). This intermediate is only 0.2 kcal/mol more stable than TS1 on the MP2/6-311+G** PES and 0.1 kcal/mol more stable on the QCISD/6-311+G** PES (see Tables 1 and 2). When the ZPVE correction from the MP2/

6-311+G** unscaled frequencies is included, this intermediate disappears from the PES.

The rate-determining TS for this elimination, TS2, is a nonplanar structure with C_s symmetry where the two leaving H atoms are equivalent (see Figure 3). In this TS2 the leaving hydrogen molecule is almost formed as the MP2 H–H distance (0.877 Å) and the presence of a BCP between the two H atoms clearly show (see Table 4). The existence of a BCP between C and H₂ located on the symmetry plane bisecting TS2 indicates that binding between the leaving hydrogen molecule and HCS⁺ corresponds to a σ–π complex¹⁰ between the two fragments. This TS2 is 61.9 kcal/mol above protonated thioformaldehyde (see Table 1). TS2 leads to H₂ + HCS⁺ products, and the computed reaction energy is 27.9 kcal/mol. No experimental data on this process were found for comparison.

For this system a C_s TS, TS3, was located (see Figure 3), which according to IRC calculations corresponds to proton scrambling between C and S atoms in protonated thioformaldehyde through the above mentioned intermediate. Interestingly, this TS3 is 56.8 kcal/mol less stable than protonated thioformaldehyde and is 5.1 kcal/mol more stable than TS2, the TS for H₂ 1,2-elimination. This situation remains practically identical when optimizing at the QCISD/6-311+G** level (see Table 2).

The H₂ elimination through a two-step mechanism via the CH–SH₂⁺ intermediate was also studied (see Figure 4). The TS for the shift of a H atom from C to S and the TS for the H₂ 1,1-elimination from the CH–SH₂⁺ intermediate are, respectively, 97.6 and 112.3 kcal/mol above protonated thioformaldehyde. None of these processes can compete with the H₂ 1,2-elimination.

Discussion

Comparing the three protonation processes studied, we see that the electronic density transference is considerably greater in the case of thioformaldehyde, which is the most readily polarizable system. Moreover, in the protonation of formaldimine and formaldehyde the added proton withdraws most of its electronic population from the hydrogen atoms attached to the carbon atom, whereas the originally positively charged S atom in thioformaldehyde becomes even more positively charged by protonation. Formaldimine, whose C–N double character remains practically unchanged after protonation (the C–N distance remains the same and the electron density at BCP decreases only 0.015 au at the MP2 level), presents the highest PA value. Formaldehyde, whose C–O double character is appreciably weakened by protonation (the C–O distance increases by 0.036 Å and the electron density at BCP decreases by 0.041 au at the MP2 level), has the lowest PA value. For thioformaldehyde the C–S double-bond character is not affected much by protonation (the C–S increases by 0.003 Å and the electronic density at BCP increases by 0.016 au at the MP2 level) and the new S–H bond is weaker than the O–H and N–H bonds, the PA presenting an intermediate value.

For the three systems investigated the H₂ 1,1-elimination paths imply high-energy barriers, and thus they are not competitive compared with the 1,2-eliminations.

The reaction paths for hydrogen 1,2-elimination from protonated formaldehyde and formaldimine are quite different according to IRC calculations. Protonated formaldehyde reaches the TS, maintaining planarity by elongation of the O–H bond and reduction of the C–O–H angle. The C–O bond distance diminishes slightly along the reaction path from reactant to TS (see Figure 1). On the contrary, the C–N bond slightly lengthens from protonated formaldimine to the TS (see Figure

2) and the reaction coordinate involves an important rotation about the C–N bond. This motion is energetically costly, an important loss of C–N double-bond character taking place in the first steps of the process. Consequently, the activation energy required to decompose protonated formalimine is greater than that to decompose protonated formaldehyde (see Tables 1 and 2).

In their detailed dynamical study of protonated formaldehyde decomposition⁴ Kim et al. found that H–C–O bending and C–O stretching were coupled with the reaction coordinate at the H₂ 1,2-elimination TS. They concluded that the contribution of these normal modes to the overall potential energy could be channeled into the reaction coordinate, explaining thus the extraordinarily large KER observed in this process. In our normal mode analysis of this TS we found that normal modes 5A' and 6A' (see Figure 5) present a certain coupling with the reaction coordinate, having a moderate value of coupling constants of 0.22 and 0.13 amu^{1/2} bohr, respectively. These normal modes account for the simultaneous H–C–O bending and C–O stretching motions, in agreement with the above mentioned study. Nevertheless, it is remarkable that, according to our calculations, the most important coupling constant ($B_{1,8} = 0.42$ amu^{1/2} bohr) corresponds to coupling between the symmetric stretching associated with the CH₂ three-center interaction (normal mode 8A') and the reaction coordinate. It is clear from Figure 5 that this normal mode will strongly contribute to the relative motion between products. No such strong coupling contributing to the relative motion of products has been detected for the other two cases by a similar normal mode analysis. In the case of protonated thioformaldehyde, a strong coupling of the reaction coordinate with the stretching of the almost formed hydrogen molecule at TS2 was found.

According to IRC calculations, the reaction path for the hydrogen elimination from protonated thioformaldehyde implies initially a rotation about the C–S bond and a simultaneous reduction of the C–S–H angle, leading to the C_s intermediate on the electronic PES. This intermediate can evolve in two different ways, reaching either TS2 for H₂ 1,2-eliminations or TS3 for proton scrambling. Comparing the three TSs for the H₂ 1,2-elimination, we see that the TS for protonated thioformaldehyde is completely different from the other two given that in the former the two leaving hydrogen atoms are equivalent, the hydrogen molecule is practically formed, and the C–S bond distance is notably shortened. Nevertheless, the most remarkable feature is the competition between proton scrambling and hydrogen elimination in protonated thioformaldehyde. According to our calculations at several levels of theory, the TS for proton scrambling in protonated thioformaldehyde is more stable than the H₂ 1,2-elimination TS by more than 5 kcal/mol (see Table 1).¹⁷ This theoretical prediction is in contrast with deuterium labeling experiments in which it has been established that CH₂SD⁺ and CD₂SH⁺ cations lose only HD. Further work seems then necessary to solve this controversy.

In summary, on protonation the electronic density transferred to the proton comes mainly from the H atoms for formaldehyde and formalimine, whereas for thioformaldehyde the contribution from the S atom is also appreciable. Only the double bond of formaldehyde is affected by protonation. Hydrogen 1,1-elimination is not competitive compared with the 1,2-elimination in all of the three cases studied. The hydrogen 1,2-elimination from protonated formaldehyde takes place maintaining planarity of the system, whereas for protonated formalimine and thioformaldehyde the reaction coordinate involves rotation about the double bond. For protonated formaldehyde, which presents the highest KER, a strong coupling was found between the reaction coordinate and the symmetric stretching of the CH₂ group, which strongly contributes to the separation of the products H₂ and HCO⁺. For protonated thioformaldehyde a TS for proton scrambling more stable than the TS for hydrogen 1,2-elimination was found, in contrast with experimental evidence.

Acknowledgment. The authors thank Dr. R. López for helpful comments and suggestions and the CICYT (Spain) for computer time on the CRAY YMP at the CIEMAT and are grateful to the DGICYT (Spain) for financial support (PB94-1314-C03-01).

References and Notes

- (1) Polanyi, J. C. *Acc. Chem. Res.* **1972**, *5*, 161–168.
- (2) Williams, D. H.; Hvistndahl, G. *J. Am. Chem. Soc.* **1974**, *96*, 6753–6755.
- (3) Uggerud, E.; Helgaker, T. *J. Am. Chem. Soc.* **1992**, *114*, 4265–4268.
- (4) Lee, T. G.; Park, S. C.; Kim, M. S. *J. Chem. Phys.* **1996**, *104*, 4517–4529.
- (5) Donchi, K. F.; Rumpf, B. A.; Willet, G. D.; Christie, J. R.; Derrick, P. J. *J. Am. Chem. Soc.* **1988**, *110*, 347–352.
- (6) Frisch, M. J.; Trucks, G. W.; Head-Gordon, M.; Hill, P. M. W.; Wong, M. W.; Foresman, J. B.; Johnson, B. G.; Schlegel, H. B.; Robb, M.; Replogle, E. S.; Gomperts, R.; Andres, J. L.; Raghavachari, K.; Binkley, J. S.; Gonzalez, C.; Martin, R. L.; Fox, D. J.; Defrees, D. J.; Baker, J.; Stewart, J. J. P.; Pople, J. A. *Gaussian 92*; Gaussian Inc.: Pittsburgh, PA, 1992.
- (7) Schlegel, H. B. *J. Comput. Chem.* **1982**, *3*, 211.
- (8) Benson, S. W. *Thermochemical Kinetics*, 2nd ed.; Wiley-Interscience: New York, 1976.
- (9) González, C.; Schlegel, H. B. *J. Phys. Chem.* **1989**, *90*, 2154.
- (10) Bader, R. F. W. *Atoms in Molecules. A Quantum Theory*; Clarendon Press: Oxford, 1990.
- (11) Biegler-König, F. W.; Bader, R. F. W.; Wang, T. H. *J. Comput. Chem.* **1982**, *3*, 317.
- (12) Miller, W. H.; Handy, N. C.; Adams, J. E. *J. Chem. Phys.* **1980**, *72*, 99.
- (13) Page, M.; McIver, J. W., Jr. *J. Chem. Phys.* **1988**, *88*, 922–935.
- (14) Smith, B. J.; Radom, L. *J. Phys. Chem.* **1995**, *99*, 6468–6471, and references therein.
- (15) Vogel, P. *Carbocation Chemistry*; Elsevier: Amsterdam, 1985.
- (16) Cremer, D.; Kraka, E. *Angew. Chem., Int. Ed. Engl.* **1984**, *23*, 627.
- (17) Grimme, S. *J. Am. Chem. Soc.* **1996**, *118*, 1529–1534.
- (17) To further investigate the effect of a greater basis set on the relative stability of TS2 and TS3, optimizations were carried out on these structures at the MP2/6-311+G(3df,2p) theory level followed by single-point calculations at the QCISD(T) level. TS3 remains 6.7 kcal/mol more stable than TS2.